Surface Science 290 (1993) 15–25
North-Holland

surface science

STM study of the structure and phases of Pb on Ge(111)

L. Seehofer, G. Falkenberg and R.L. Johnson
II. Institut für Experimentalphysik, Universität Hamburg, Luruper Chaussee 149, D-2000 Hamburg 50, Germany

Received 25 November 1992; accepted for publication 10 February 1993

The different structures of Pb on Ge(111) have been studied as a function of Pb-coverage up to two monolayers with scanning tunneling microscopy. At low coverages a $c(2 \times 8)$ and a $(\sqrt{3} \times \sqrt{3})$R30° reconstruction with a mixture of Pb and Ge adatoms both occupying T4-sites was observed. The bias voltage dependence of topographic images of these structures is interpreted in terms of a charge transfer between the different adatom dangling-bond orbitals. On the basis of the STM images new structural models for the metastable (4×4) reconstruction and the higher density $(\sqrt{3} \times \sqrt{3})$R30° reconstruction are proposed. In addition a previously unobserved striped incommensurate phase was found for coverages greater than 4/3 monolayers. The data from this striped phase are compared with the predictions of domain-wall theory for commensurate–incommensurate phase transitions.

1. Introduction

The closely-related systems Pb/Ge(111) and Pb/Si(111) may be considered as prototype models of simple metal–semiconductor interfaces because in both cases abrupt junctions with negligible intermixing are formed. The solubility of Pb in bulk Si and Ge is extremely small and there are no chemical reactions between the components [1]. The Schottky-barrier height of Pb/Si(111) diodes is known to be strongly dependent on the epitaxial orientation of the first Pb monolayer [2,3]. Hence, studies of the atomic geometry of Pb–semiconductor interfaces should provide some insight into the mechanisms that determine Schottky-barrier heights. Furthermore, since Pb neither desorbs from nor diffuses into the substrate over a wide range of temperatures, ideal Pb/Ge(111) and Pb/Si(111) interfaces are experimental realisations of 2D systems which can be used to test the range of applicability of the theory of critical phenomena in two dimensions. For example, Pb/Ge(111) displays a reversible phase transition which has been interpreted as a 2D melting process [4,5]. Consequently the structure and physical properties of Pb/Ge(111) are of considerable interest for both technological and fundamental reasons.

The surface structure of Pb/Ge(111) was first studied by Metois and Le Lay using low energy electron diffraction (LEED), Auger electron spectroscopy and scanning electron microscopy in 1983 [6]. They identified three $(\sqrt{3} \times \sqrt{3})$R30° structures (in the following referred to as $\sqrt{3}$) at coverages of 0.03, 0.3 and 1 ML, where one monolayer (ML) is equal to 7.22×10^{14} atoms/cm^2. Ichikawa proposed a phase-diagram for Pb/Ge(111) based on reflection high energy electron diffraction (RHEED) measurements [7]. In addition to a metastable (4×4) reconstruction two different $\sqrt{3}$ structures were found; the α-(dilute) phase and the β-(dense) phase. The structural models for the $\sqrt{3}$ structures of Pb/Ge(111) derived from surface X-ray diffraction (XRD) experiments [8] are similar to the original model proposed by Estrup and Morisson [9] for Pb/Si(111): i.e., a simple adatom model formed by placing the Pb-atoms above the second-layer Ge-atoms (T4-sites) in the α-phase and a single distorted close-packed 30° rotated Pb-layer with only 1% mismatch to an ideal Pb(111) layer in the β-phase. The corresponding saturation coverages

are 1/3 and 4/3 ML respectively. X-ray standing wave measurements (XSW) [10] and dynamical LEED analysis [11] revealed that the lead atoms of the close-packed β-phase form a double layer. Recently a $\sqrt{3}$ mosaic phase was observed for Sn and Pb on Si(111) [11]. Based on scanning tunneling microscopy (STM), LEED, Rutherford backscattering (RBS) and thermal desorption spectroscopy Ganz et al. proposed that the mosaic phase of Pb/Si(111) consists of alternating chains of Pb and Si adatoms on T4-sites (1:1 Pb to Si ratio) giving a coverage of 1/6 ML of Pb [13]. Ganz et al. also used STM to study the surface diffusion of isolated Pb adatoms on Ge(111) [14]. In the following we report results from STM measurements on the geometrical structures of Pb on Ge(111) in the coverage regime up to two monolayers.

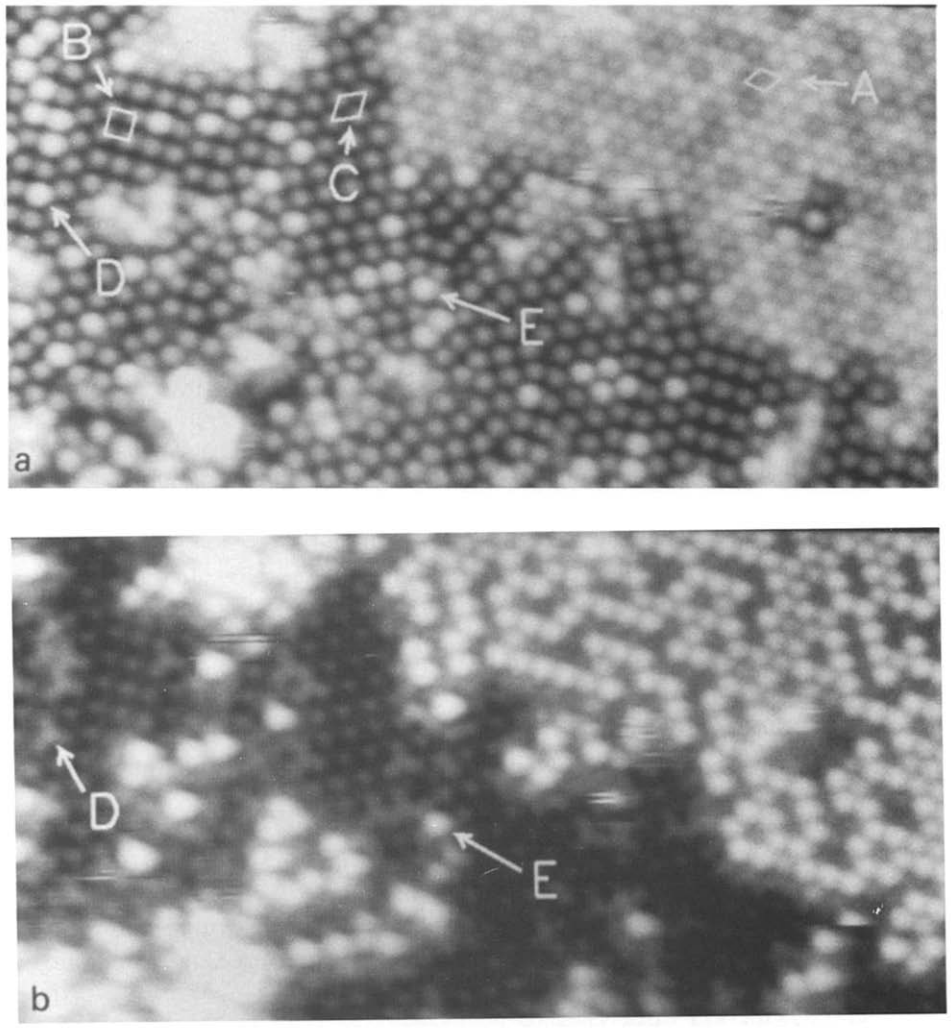

Fig 1. Tunneling image of a 290 × 150 Å^2 area of 0.1 ML Pb on Ge(111) acquired at (a) +1.2 V sample bias and 1.5 nA tunneling current (b) −1.0 V sample bias and 1.3 nA tunneling current. The arrows indicate $\sqrt{3}$ (A), c(2 × 4) (B) and (2 × 2) (C) unit cells and two separate Pb adatoms (D and E).

2. Experimental

The experiments were performed in an ultra high vacuum (UHV) system (base pressure $< 4 \times 10^{-11}$ mbar) consisting of a molecular beam epitaxy deposition chamber equipped with a RHEED apparatus, sample heating and a quartz film-thickness monitor, a separate preparation chamber for sputtering and annealing to clean the substrates and an analysis chamber containing a LEED system and a commercial STM (OMICRON Vakuumphysik GmbH). We used electrochemically etched tungsten tips, which were formed in situ by scanning at high bias voltage and tunneling current. If not otherwise mentioned all images shown here are unfiltered raw data with a linear background subtracted. Clean reconstructed Ge(111)-c(2 × 8) surfaces were prepared by repeated cycles of sputtering with 500 eV Ar^+ ions at a temperature of 500°C and annealing at 650°C until a bright and sharp c(2 × 8) LEED pattern with a low background was observed. The duration and temperature of the annealing process as well as the cooling rate after the anneal do not seem to be particularly critical parameters. STM images of the clean Ge(111)-c(2 × 8) surface showed large terraces (~ 5000 Å)^2 of c(2 × 8) structure with a domain size of typically (500 Å)^2. Images of the clean reconstructed Ge surface at a small negative bias voltage were used to determine the orientation of the sample. Pb was evaporated from an effusion cell with a PBN crucible at a rate of $\sim 5 \times 10^{-3}$ ML/s. During deposition the pressure was maintained at less than 1×10^{-10} mbar. We found that samples could be cleaned for reuse either by sputtering and annealing or by simply heating up to 500°C to desorb all of the Pb.

3. Results and discussion

We begin by presenting our results for low coverages deposited at room temperature. After depositing about 0.1 ML Pb we observed an electron diffraction pattern consisting of c(2 × 8) and weak $\sqrt{3}$ spots. STM images from the same sample showed large c(2 × 8) reconstructed domains with a few bright protrusions, typically one per (100 Å)^2, probably caused by single lead atoms. Most of the lead seemed to be concentrated at steps and domain boundaries of the c(2 × 8) reconstruction in areas which had a diffuse and foggy appearance in the STM images. Sometimes we observed a faint $\sqrt{3}$ pattern inside these structures. During the first seconds of a short anneal at about 100°C the $\sqrt{3}$ RHEED pattern became brighter and less streaky. STM topograms showed that after annealing the lead atoms were distributed more uniformly over the sample and that most of the lead atoms had replaced Ge adatoms. We conclude that at room temperature the lead atoms generally do not have enough energy to displace the Ge adatoms so they are losely bound and highly mobile on the undisturbed reconstructed Ge surface. The high mobility of the lead atoms leads to the formation of clusters at any kind of defects such as step edges, and if the local density of Pb atoms is high enough a $\sqrt{3}$-phase will develop. If not otherwise mentioned the following results were obtained from samples which were annealed for about 5 min at 100°C after deposition at room temperature.

In fig. 1 two tunneling topograms from a sample with a coverage of about 0.1 ML are shown which were acquired at bias voltages of +1.2 and −1.0 V, respectively. The imaged surface consists basically of two parts; on the right there is a $\sqrt{3}$-reconstructed area while in the rest of the image, which is less well ordered, one can see mainly the two types of unit cells which form the building blocks of the c(2 × 8) reconstruction of clean germanium, i.e., c(2 × 4) and (2 × 2) units [15,16]. Within these unit cells both grey (e.g. at B and C) and white (e.g. at D and E) protrusions can be seen with positive sample bias. The coverage dependence of these protrusions indicates that the white protrusions are due to Pb atoms and the grey protrusions correspond to Ge atoms. It is well known that STM images of the clean Ge(111)-c(2 × 8) surface reveal two different types of surface atoms, namely the adatoms at T4-sites and the triply-coordinated second-layer rest-atoms which have an unsaturated dangling bond [17]. Since there is a charge transfer in the c(2 × 8) reconstruction from the Ge adatoms to the Ge

rest-atoms the dangling-bond band of the adatoms is almost empty while the rest-atom dangling-bond band is almost completely filled [17–19]. Accordingly the darker protrusions in the empty-state image (fig. 1a) correspond to the Ge adatoms located at T4-sites and it is easy to verify directly from the STM images that the Pb atoms as well as the protrusions in the $\sqrt{3}$-reconstructed area are also located at T4-sites. At a bias of -1.0 V the Ge rest-atoms become visible instead of the adatoms. The Pb adatoms can still be seen, but some of them appear as bright as the white protrusions in the $\sqrt{3}$-reconstructed area (E) and some of them appear darker (D). We can explain this assuming that there is charge transfer from the Pb atoms of type D to the neighbouring Ge rest-atoms. The appearance of the type E Pb atoms can be explained by a blocking of the charge transfer which may have several possible causes. The most obvious reason for the charge transfer to be blocked is when there are no neighbouring rest-atoms, or an insufficient number of neighbouring rest-atoms as is the case for the atom marked (E) which is located at the corner of a single $\sqrt{3}$ unit cell. Other possible mechanisms for blocking of charge transfer such as hydrogen contamination or Group III impurities have recently been discussed in two studies concerning charge transfer in the clean Ge surface [20,21].

In the $\sqrt{3}$-reconstructed part of the filled-state image (fig. 1b) bright protrusions and darker spots can be seen. At higher Pb coverage the number of dark spots decreases (see fig. 2a) so we conclude that the bright protrusions are due to type E Pb adatoms while the dark spots are caused by Ge adatoms which are incorporated into the new reconstruction. We find that all of the atoms are located at T4-sites, in good agreement with the model proposed by Feidenhans'l et al. from X-ray diffraction studies [8] which is also supported by theoretical calculations [22]. In the filled-state image 2a and in the corresponding cross-section (2b solid line) it can be seen that there is an indentation at the position of the Ge atoms and that the adjoining Pb atoms appear (0.1–0.2) Å higher than the other Pb atoms. In the cross-section taken from the corresponding image at positive bias (fig. 2b dashed line) the indentation at the position of the Ge atoms has changed into a protrusion which is, however, still smaller than that of the Pb atoms. We can explain this assuming that, since the Pb atoms have a larger covalent radius, they are higher than the embedded Ge atoms and that there is charge transfer from the Ge adatoms to the neighbouring Pb adatoms. This charge transfer leads to an enhanced contrast in the apparent height between the two types of atoms for negative bias and to a reduced contrast at positive bias. A similar charge transfer has been reported in a recent photoemission study

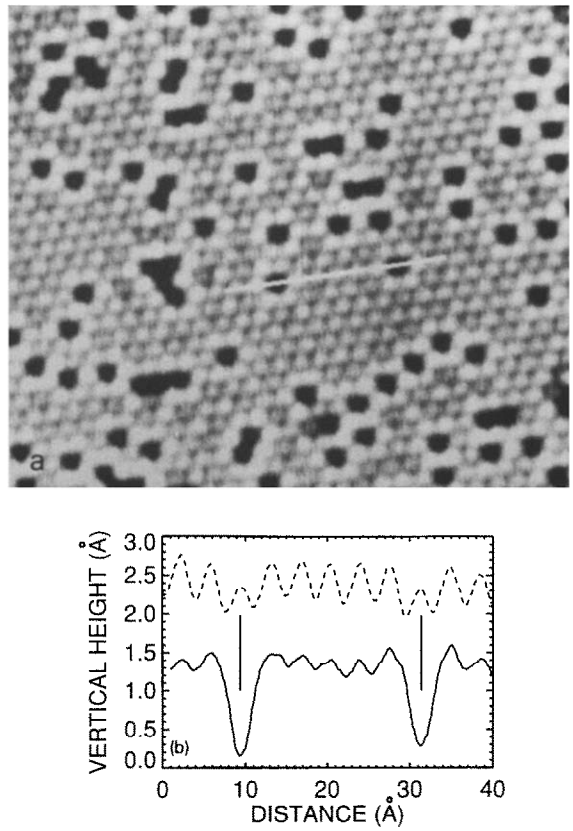

Fig. 2. (a) STM image of a 325×350 Å^2 area of the α-phase of Pb/Ge(111) acquired with a sample bias of -0.6 V and 1.0 nA tunneling current. (b) Cross-sections taken along the high-lighted line in (a) (solid line) and along the same line in a corresponding empty-state image acquired with a sample bias of $+1.2$ V and a tunneling current of 2.1 nA (dashed line). The two vertical lines indicate the positions of substitutional Ge adatoms.

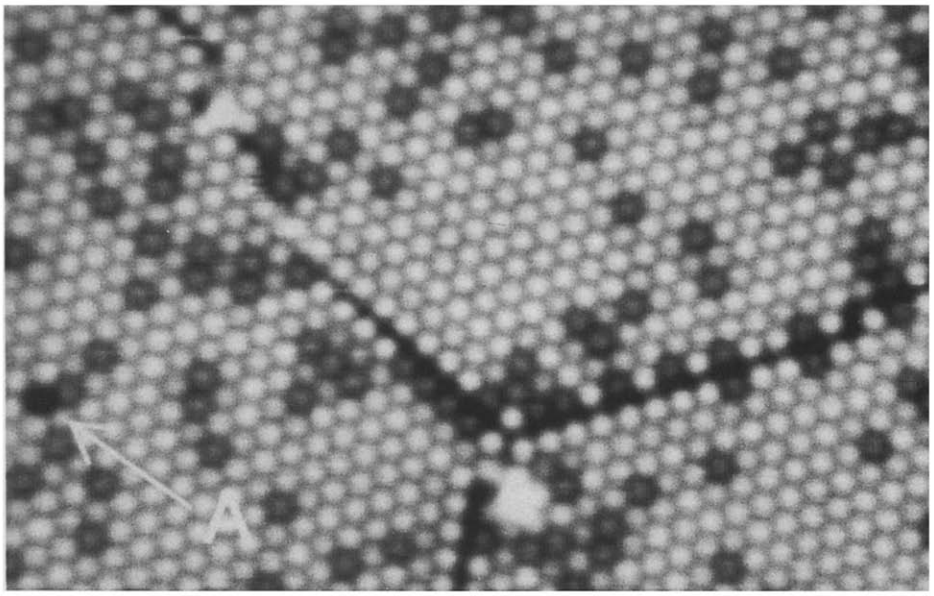

Fig. 3. Tunneling image of a 230×150 Å^2 area of the $\sqrt{3}$ α-phase of Pb/Ge(111) acquired with a sample bias of $+1.0$ V and a tunneling current of 1.0 nA. The three sub-domains are separated by domain boundaries consisting mostly of primitive c(2×4) unit cells. The arrow (A) indicates a vacancy.

of the mosaic phase of Pb/Si(111) [23]. In fig. 1b it can be seen that the different atoms are not distributed randomly, but tend to form chains. Similar chains have also been observed for Pb/Si(111) [13] and Al/Si(111) [24] and it has been suggested that such structures may be inter-

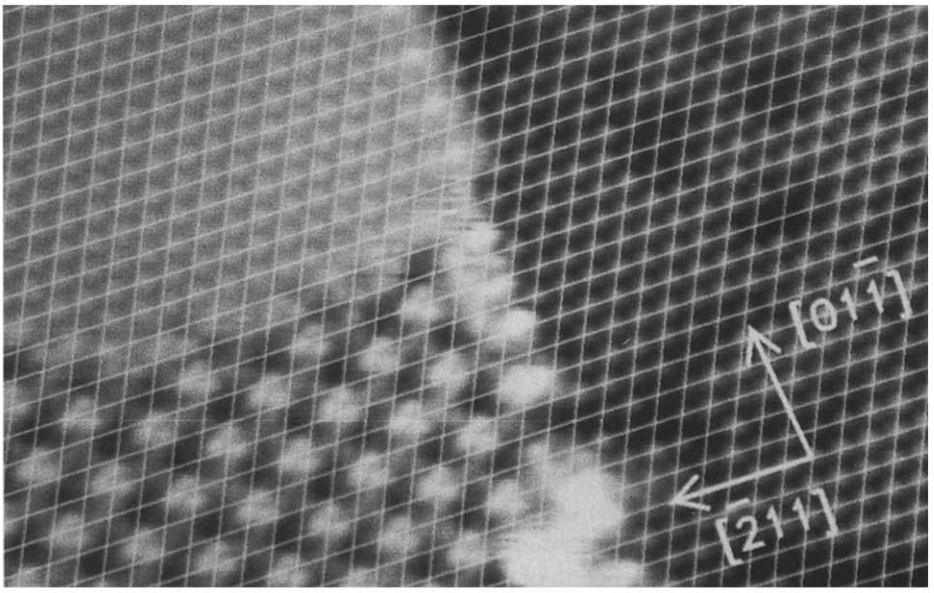

Fig. 4. STM image acquired at $+1.0$ V sample bias and 1.0 nA tunneling current from a 220×150 Å^2 area of a Ge surface covered with ~ 0.5 ML Pb. The α-phase is on the right, the β-phase in the upper-left corner and the metastable (4×4) reconstruction in the lower-left corner. The superimposed $\sqrt{3}$ grid is in registry with the α-phase.

preted by analogy with a two-dimensional hexagonal antiferromagnetic Ising model [13]. Such an interpretation is hampered by the fact that the charge transfer and consequently also the interaction between the atoms depends on the environment of each atom.

At coverages close to 1/3 ML almost the entire surface is covered with the $\sqrt{3}$ α-phase with a few remaining substitutional Ge adatoms. Domain sizes are typically (100–300 Å)^2 and domain boundaries consisting mostly of primitive c(2 × 4) unit cells are formed (see fig. 3). The number of point defects (e.g. at A) found on the surface was very small. They may be attributed to either vacancies or contamination with hydrogen atoms which modify the surface electronic structure by saturating dangling bonds.

At coverages above 1/3 ML two new surface structures, a metastable (4 × 4) reconstruction and the close-packed $\sqrt{3}$ β-phase, begin to develop. In fig. 4 which is an empty-state image from a sample with a coverage of about 0.5 ML, both $\sqrt{3}$-phases can be seen in coexistence with the (4 × 4) reconstruction. The superimposed grid was aligned with the α-phase on the right. In the β-phase shown in the upper-left corner of the image, one protrusion per unit cell can be seen which is located for both tunneling voltage polarities on a hollow site above the fourth Ge layer (H3). The corrugation observed on the β-phase for negative tunneling voltages was typically 0.05 Å which is much smaller than that of the α-phase. The occupied states in the β-phase are therefore delocalized as in metals, whereas the bonding in the α-phase is more covalent in nature. Depending on the bias and the conditions of the tip the β-phase lies between 1 and 1.6 Å higher than the α-phase. In fig. 5a an STM topogram of the β-phase recorded with a bias voltage of +5.0 mV and a tunneling current of 12 nA is shown. Now four protrusions per unit cell can be seen which can be mapped onto the Ge substrate lattice as shown in fig. 5b. This picture is quite similar to the structural model of the β-phase derived from X-ray diffraction [8]. The main difference is that we have rotated the substrate 180° around the surface normal which places the bridge-site atoms closer to T4-sites instead of T1-sites. This gives a more plausible picture for the growth of the β-phase because in our model we can obtain the β-phase from the α-phase by simply filling in the interstitial positions. In our STM topograms the hollow-site atoms appear ~0.15 Å higher than the bridge-site atoms. We obtain a closest in-plane distance between Pb atoms of $a = (2.9 \pm 0.2)$ Å which agrees well with the value from X-ray diffraction of (3.11 ± 0.02) Å [8].

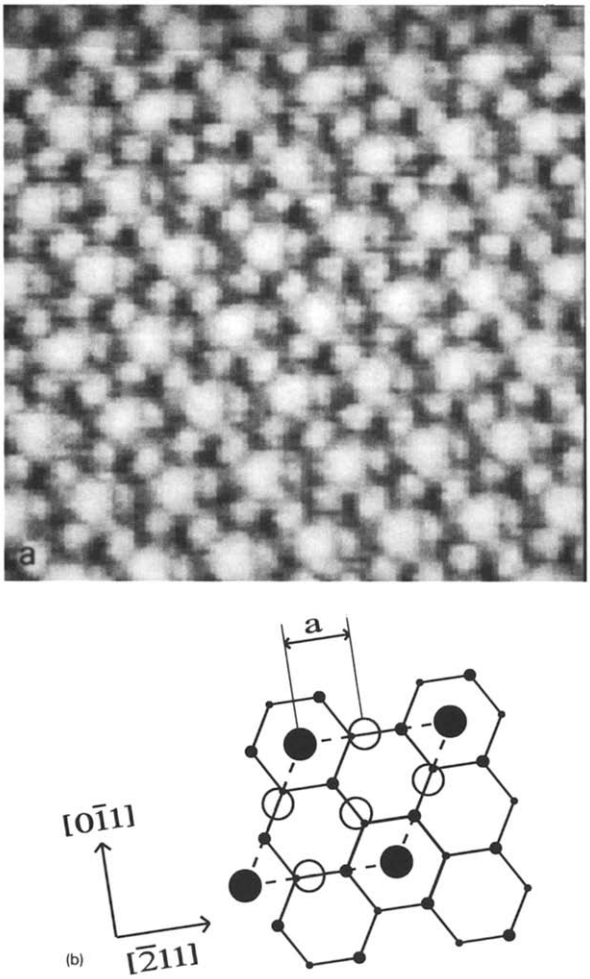

Fig. 5. (a) Tunneling image of a 50×50 Å^2 area of the β-phase acquired with +5.0 mV sample bias and 13 nA tunneling current. (b) Structural model of the β-phase. Small and medium sized filled circles represent the ideal (111) surface. The dashed lines indicate a $\sqrt{3}$ unit cell. Large open circles represent Pb atoms occupying bridge positions close to T4-sites and the large filled circles represent Pb atoms at H3-sites.

In the (4×4)-reconstructed part of the surface six protrusions per unit cell can be seen. Assuming that each protrusion represents a Pb atom we obtain the structural model for the (4×4) reconstruction shown in fig. 6. The model corresponds to a coverage of 9/24 ML, which is slightly greater than the 8/24 ML saturation coverage of the α-phase. The protrusions marked as filled circles in fig. 6 appear higher in a filled-state image (not shown), while the open circles mark the brightest spots in the empty-state image (fig. 4). The domain sizes which we obtained with our preparation technique were typically only (100–400 Å)^2. The domains were separated by $\sqrt{3}$-reconstructed areas and we never observed a subdomain boundary inside the (4×4) areas. On heating the sample up to 300°C the (4×4) reconstruction vanished completely and irreversibly. A detailed analysis of the (4×4) reconstruction will be presented elsewhere.

At a coverage of 1.3 ML the whole surface is covered by the $\sqrt{3}$ β-phase. Adding more lead to the sample gives rise to a striped incommensurate structure (SIC) which to our knowledge has not been observed previously in this system. The driving force for the formation of a SIC arises from the competition between the inter–adatom and the adatom–substrate interactions. The basic ideas for the theoretical description of commensurate–incommensurate (CI) phase transitions go back to the 1D model of Frank and van der Merwe [25]. They calculated that the ground state of an adlayer at a coverage slightly above or below the commensurate value should consist of broad commensurate regions separated by narrow regions with a correspondingly higher or lower density, which are called misfit dislocations, solitons or domain walls. The theoretical description of such systems has attracted considerable attention over the past twenty years and a vast amount of literature has accumulated [26]. For a system with hexagonal symmetry Bak et al. [27] determined two possible kinds of domain networks at zero temperature depending on the energy of the wall intersections and on the misfit between substrate and adsorbate layer; a striped phase (SIC) consisting of parallel domain walls and a hexagonal phase (HIC) in which the domain walls form a honeycomb pattern. They showed that the commensurate–incommensurate phase transition should be first order for the HIC while a transition to a SIC should be continuous. At elevated temperature the domain walls are expected to meander and intersections of the walls also become possible in the striped phase [28].

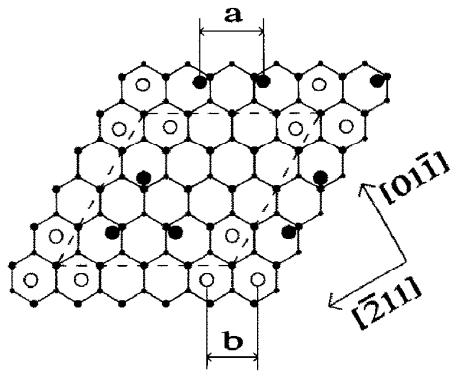

Fig. 6. Structural model of the (4×4) reconstruction. Small and medium-sized filled circles represent the ideal (111) surface. The dashed lines indicate a (4×4) unit cell. Large open circles represent Pb atoms which appear bright in empty-state images while the Pb atoms represented by large filled circles appear bright in filled-state images ($a = 6.0 \pm 0.7$ Å, $b = 4.5 \pm 0.4$ Å).

Most experimental data on CI phase transitions have so far been obtained using diffraction techniques [29]. The first direct observation of domain walls was on 2H–$TaSe_2$ in 1981 using electron microscopy [30]. Domain walls can be characterized by four quantities: displacement vector, width, direction and the excess density compared to the commensurate value per unit length. The first three of these quantities can be obtained easily with STM, which is not the case for diffraction methods or conventional electron microscopy. The displacement vector of the domain walls is a topological feature for each wall, which is independent of the direction of the wall, and must be a lattice vector of the substrate. In other words a domain wall separates two of the equivalent sub-domains of the adsorbate-induced structure. A $\sqrt{3}$ structure has three subdomains as illustrated in fig. 7b. (Rare gases adsorbed on graphite, which also have $\sqrt{3}$ structures, have in

the past served as model systems for testing domain-wall theory. Since many result of the theory only depend on the symmetry of the system we can directly compare our measurements to theory.) Fig. 7a shows a tunneling topogram of a sample with a lead coverage of approximately 1.4 ML, which incidentally was not very well prepared since it has a lot of defects. The sub-domains are labelled according to fig. 7b. At two points one can see three intersecting domain walls separating all three subdomains. For samples with less defects very few wall intersections were found which indicates that firstly Pb on Ge gives rise to a striped incommensurate phase and secondly the domain walls can be pinned by defects. The width of a single domain wall is about 66 Å and is independent of the coverage. We found that the domain walls tend to run almost parallel to a $[11\bar{2}]$ direction. The typical distance between two domain walls depends on the coverage and reaches a minimum of about 130 Å at coverages above 1.6 ML. Adding more lead to the sample does not change the appearance of the domain walls in STM, but the LEED pattern indicates the presence of 3D lead crystallites. Each domain wall looks like a herring-bone pointing in $[\bar{1}\bar{1}2]$ direction with a hexagonal structure in the middle with protrusions located at

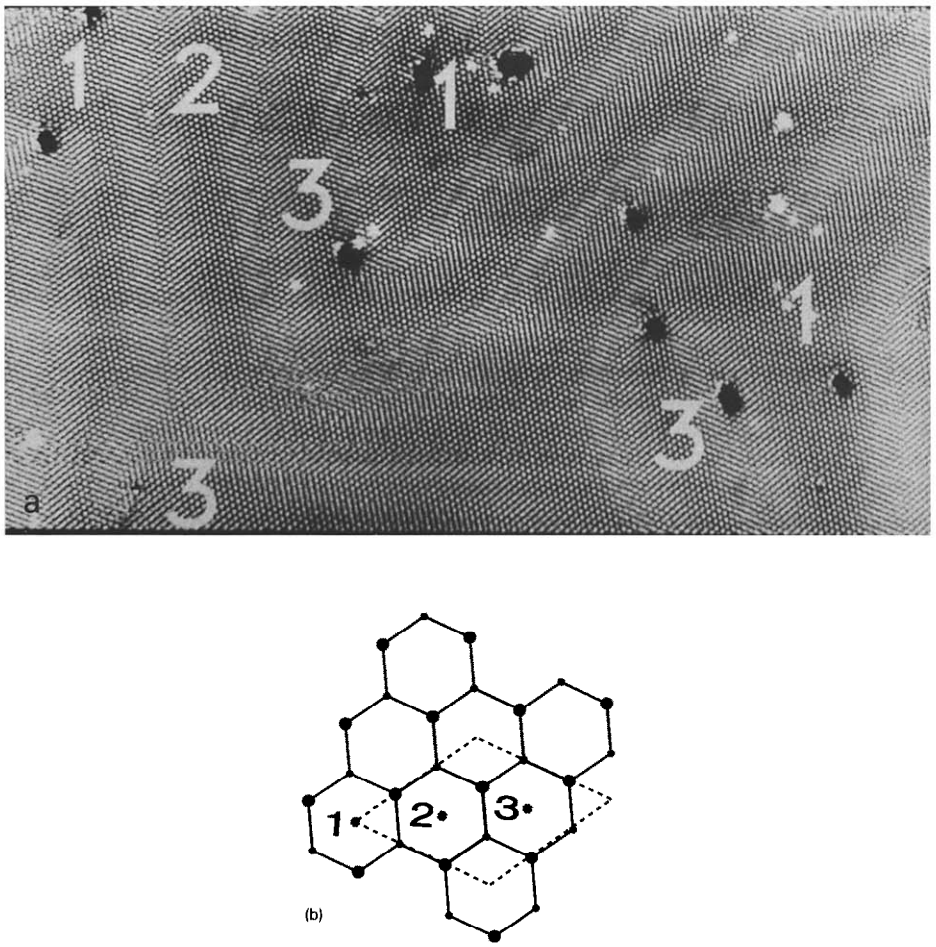

Fig. 7. (a) STM image acquired at +0.16 V sample bias and 1.6 nA tunneling current from a 980×560 Å^2 area of a Ge surface covered with ~ 1.4 ML Pb. The sub-domains are labeled according to (b). (b) Ideal (111) surface with a $\sqrt{3}$ unit cell (dashed). The asterisks indicate the origins of the three different subdomains of the $\sqrt{3}$ structure.

T4-sites. One possibility for calculating the excess density of the domain walls is simply to use the displacement vector [31] which would indicate that the walls are of the superheavy type as shown in fig. 7a. This picture seems to be too simplistic since, in our case, the fact that the protrusions in the hexagonal structure in the middle of the domain walls are located at T4-sites indicates that the walls are not formed by a simple uniaxial compression of the commensurate phase perpendicular to the direction of the walls. Obviously the symmetry of the substrate which is C_{3v} in this case and not hexagonal plays a role in the sense that T1- and T4-sites are inequivalent. We think that the additional mass in the domain walls sits adjacent to the hexagonal structure giving rise to the "bones". One needs a detailed atomic model of the domain walls to determine the excess density and this information is not available at present.

We frequently observed, as in the lower left corner of fig. 7a, that the domain walls are less stable at kinks or at intersections between the walls since tunneling conditions were often unstable at these points. This effect together with the protrusions being in the middle of the walls are both in agreement with the fact that one observes a striped and not a honeycomb phase. Assuming that the protrusions in the middle of the domain walls correspond directly to the positions of lead atoms one can argue as follows. At an intersection of three domain walls, each wall would like to shift a Pb adatom to a different T4-site corresponding to the three different domains giving rise to an unstable structure which is energetically unfavourable. Consequently the system tries to minimize the number of wall intersections and kinks which leads to a striped phase. Since we never observed a striped phase in coexistence with the commensurate β-phase and since the distance between the domain walls is a continuous function of the coverage we believe that the CI phase transition of Pb/Ge(111) is continuous, in agreement with the theory of Bak et al. [27]. The domain walls run mostly parallel to step edges; although, if they end at a step edge, they approach it almost perpendicularly.

No differences were found between samples which were not annealed after depositing over 1.4 ML Pb at room temperature and those annealed at 100°C. However, after heating the SIC phase above the $\sqrt{3}$ to 1×1 phase transition temperature we only observed a pure β-phase with STM. The additional lead probably diffused into the 3D lead crystallites which were identified in LEED. On the time scale of hours we did not observe any movement of domain walls at room temperature. It should be noted that at this level the continuous approximation for the overlayer is no longer adequate and one has to take the discreteness of the overlayer into account which leads to a pinning of the domain walls even on the defect-free ideal surface [28]. Consequently, our measurements taken at room temperature primarily reflect the $T = 0$ case for which no wall intersections are predicted, which supports the idea that the intersections observed are caused by finite-size effects and an additional pinning of the walls at defects.

We have demonstrated that in the β-phase of Pb/Ge(111) the domain walls are the primary location of the excess density over the commensurate phase. Now it is worth considering the saturated α-phase again (fig. 3) where the situation is

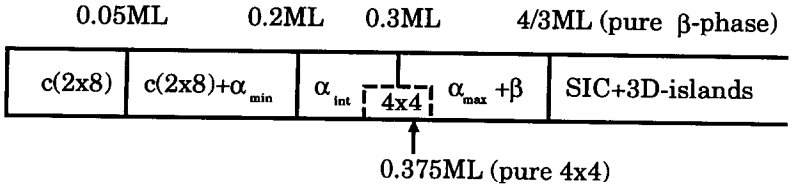

Fig. 8. Experimental phase diagram for the room temperature phases of Pb/Ge(111).

reversed. If we simply ignore that we have two different kinds of adatoms we obtain an average adatom density which is below the commensurate value. However, in this case most of the missing adatom density is concentrated in the three intersecting light domain walls

Fig. 8 shows a simple one-dimensional phase diagram for Pb/Ge(111) derived from our experimental data. We determined the first three coverages by counting the different sorts of adatoms in 28 STM images with a typical size of (500 Å)^2. The values were reproducible for different samples within an error of a few percent. The last coverage given was determined from the ideal value for a $\sqrt{3}$ structure with four atoms per unit cell. Up to a coverage of 0.05 ML we only observed the c(2 × 8) structure with poor long-range order which consists of a mixture of Pb and Ge adatoms. From 0.05 ML to 0.2 ML we found the c(2 × 8) reconstruction in coexistence with the α-mosaic phase. The lowest fraction of Pb adatoms in the mosaic phase, corresponding to a coverage of (0.200 ± 0.015) ML, was observed if the mosaic phase was in coexistence with the c(2 × 8) reconstruction. The corresponding maximum value for the mosaic phase in coexistence with the β-phase was (0.297 ± 0.006) ML. All intermediate values were possible if the α-phase was alone or in coexistence with only the (4 × 4) reconstruction. It should be noted that our minimum value for the lead coverage of the mosaic phase is slightly higher than the value of 1/6 ML for Pb/Si(111) determined by Ganz et al. [13] using RBS. Since we find that over a wide range of coverages the α-phase always has incorporated Ge atoms, it seems likely that if more lead is added to the sample the displaced Ge atoms are able to move large distances over the surface and will probably agglomerate at step edges. In the β-phase, on which we observed very few point defects, we often found almost circular islands of α-phase with diameters of typically 200–300 Å. At coverages above 4/3 ML we observed similar islands of β-phase on the striped phase and also striped phase islands on the striped phase. Since we never saw similar islands on the clean germanium surface, or on the α-phase, we conclude that these islands are formed from Ge atoms which were previously substitutional adatoms in the mosaic phase which were trapped by the growing β-phase.

The coverage range over which we observed the (4 × 4) reconstruction is also marked in the phase diagram. The coverage of 0.375 ML corresponds to the ideal value for a (4 × 4) structure with six atoms per unit cell as in the structural model shown in fig. 4b.

4. Conclusions

We have examined in detail the different structures of Pb on Ge(111) as a function of coverage in the region up to two monolayers. The c(2 × 8) and the $\sqrt{3}$ α-phase reconstructions found at low coverages can both be described by a simple adatom model with T4 adsorption sites. In both reconstructions Pb and Ge adatoms can replace each other which contrasts to the extremely low bulk solubility of Pb in Ge. In the c(2 × 8) phase there is charge transfer from the Pb adatoms to the Ge rest-atoms, while in the $\sqrt{3}$ α-phase the charge transfer is from the Ge adatoms to the Pb adatoms. In the α-phase we observed frequent domain boundaries consisting mostly of primitive c(2 × 4) unit cells. We have suggested a new structural model for the metastable (4 × 4) structure found at intermediate coverages and a modified structural model for the close-packed $\sqrt{3}$ β-phase. Finally, above the saturation coverage of the β-phase we observed a striped incommensurate phase which can be described in terms of domain-wall theory. The width of the domain walls is about 66 Å and they are mostly oriented in the [11$\bar{2}$] direction.

Acknowledgement

The financial support of the Volkswagen Stiftung under project no. I/65 092 is gratefully acknowledged.

References

[1] R.P. Elliott, Constitution of Binary Alloys, 1st Suppl. (McGraw Hill, New York, 1965).

[2] D.R. Heslinga, H.H. Weitering, D.P. van der Werf, T.M. Klapwijk and T. Hibma, Phys. Rev. Lett. 64 (1990) 15893.
[3] G. Le Lay and K. Hricovini, Phys. Rev. Lett. 65 (1990) 807.
[4] T. Ichikawa, Solid State Commun. 49 (1984) 59.
[5] F. Grey, Thesis Copenhagen University, Risø National Laboratory, ISBN 87-550-1454-2 (1988).
[6] J.J. Metois and G. Le Lay, Surf. Sci. 133 (1983) 422; G. Le Lay and J.J. Metois, Appl. Surf. Sci. 17 (1983) 131.
[7] T. Ichikawa, Solid State Commun. 46 (1983) 827.
[8] R. Feidenhans'l, J.S. Pedersen, M. Nielsen, F. Grey and R.L. Johnson, Surf. Sci. 178 (1986) 927; J.S. Pedersen, R. Feidenhans'l, M. Nielsen, F. Grey and R.L. Johnson, Surf. Sci. 189/190 (1987) 1047.
[9] P.J. Estrup and J. Morrison, Surf. Sci. 2 (1964) 465.
[10] B.N. Dev, F. Grey, R.L. Johnson and G. Materlik, Europhys. Lett. 6 (1988) 311.
[11] H. Huang, C.M. Wei, H. Li, B.P. Tonner and S.Y. Tong, Phys. Rev. Lett. 62 (1989) 559.
[12] J.A. Kubby, Y.R. Wang and W.J. Greene, Phys. Rev. Lett. 65 (1990) 2165.
[13] E. Ganz, F. Xiong, I.-S. Hwang and J. Golovchenko, Phys. Rev. B 43 (1991) 7316; E. Ganz, I.-S. Hwang, F. Xiong, S.K. Theiss and J. Golovchenko, Surf. Sci. 257 (1991) 259.
[14] E. Ganz, S.K. Theiss, I.-S. Hwang and J. Golovchenko, Phys. Rev. Lett. 68 (1992) 1567.
[15] R. Feidenhans'l, J.S. Pedersen, J. Bohr, M. Nielsen, F. Grey and R.L. Johnson, Phys. Rev. B 38 (1988) 9715.
[16] R.S. Becker, J. Golovchenko and B.S. Swarzentruber, Phys. Rev. Lett. 54 (1985) 2678.
[17] R.S. Becker, B.S. Swarzentruber, J.S. Vickers and T. Klitsner, Phys. Rev. B 39 (1989) 1633.
[18] R.D. Meade and E. Vanderbilt, Phys. Rev. B 40 (1989) 3905.
[19] J.M. Nicholls, B. Reihl and J.E. Northrup, Phys. Rev. B 35 (1987) 4137.
[20] T. Klitsner and J.S. Nelson, Phys. Rev. Lett. 67 (1991) 3800.
[21] P. Molinàs-Mata and J. Zegenhagen, to be published.
[22] J.M. Carter, V.M. Dwyer and B.W. Holland, Solid State Commun. 67 (1988) 643.
[23] C.J. Karlsson, E. Landemark, Y.-C. Chao and R.I.G. Uhrberg, Phys. Rev. B 45 (1992) 6321.
[24] R.J. Hamers, J. Vac. Sci. Technol. A 6 (1988) 1462.
[25] F.C. Frank and J.H. van der Merwe, Proc. Roy. Soc. London 198 (1949) 205.
[26] See, e.g., P. Bak, Rep. Prog. Phys. 45 (1982) 587; P. Bak, in: Chemistry and Physics of Solid Surfaces V, Eds. R. Vanselow and R. Howe (Springer, Heidelberg, 1984); J. Villain and M.B. Gordon, Surf. Sci. 125 (1983) 1, and references therein.
[27] P. Bak, D. Mukamel, J. Villain and K. Wentorska, Phys. Rev. B 19 (1979) 1610.
[28] See, e.g., V.L. Pokrovsky, Helv. Phys. Acta 56 (1983) 677, and references therein.
[29] See, e.g., K. Kern and G. Comsa, in: Chemistry and Physics of Solid Surfaces VII, Eds. R. Vanselow and R. Howe (Springer, Berlin, 1988); S.K. Sinha, in: Methods of Experimental Physics, Vol. 23 B, Eds. K. Sköld and D.L. Price (Academic Press, Orlando, 1987) p. 1, and references therein.
[30] K.K. Fung, S. McKernan, J.W. Steeds and J.A. Wilson, J. Phys. C 14 (1981) 5417.
[31] See, e.g., M. den Nijs, in: Phase Transitions and Critical Phenomena, Vol. 12, Eds. C. Domb and J.L. Lebowitz (Academic Press, London, 1988), and references therein.